



ELSEVIER

Applied Mathematical Modelling 24 (2000) 131–145

APPLIED  
MATHEMATICAL  
MODELLING

www.elsevier.nl/locate/apm

# Dynamic model for predicting dust-borne odour concentrations in ventilated animal housing

Chung-Min Liao<sup>\*</sup>, Jui-Sheng Chen, Jein-Wen Chen

*Department of Agricultural Engineering, National Taiwan University, Taipei 10617, Taiwan, ROC*

Received 15 June 1998; received in revised form 11 May 1999; accepted 7 June 1999

---

## Abstract

The behavior of the interaction among odour, airborne dust, and dust-borne odour in a ventilated enclosure was studied from a dynamic point of view. Various parameters are of interest including the odour emission from stored manure, the role of ventilation as a removal mechanism, and the behavior of the ambient airborne dust present in the animal housing. Gas-phase (odour), airborne dust-phase, and adsorbed-phase (dust-borne odour) were included in the model to reflect the dynamic and time-dependent scheme such as odour degradation, adsorption of odour to the existing airborne dust, ventilation, and surface deposition. The derived dynamic equations are sufficiently general to take into account the simultaneous removal effects of turbulent diffusive deposition, gravitational sedimentation, and airflow within a ventilated enclosure. A sensitivity analysis for evaluating the parameters such as ventilation rate, dust particle size, and ambient aerosol profile is also presented. The model can be used in the future to evaluate the dust-borne odour exposure as a function of environmental and other parameters such as aerosol profile, ventilation rate, and enclosure dimension. © 2000 Elsevier Science Inc. All rights reserved.

*Keywords:* Airborne dust; Adsorption; Deposition; Dust-borne odour; Odour

---

## 1. Introduction

Odour from livestock manure is a complex mix of organic and inorganic compounds. To evaluate the significance of this contribution to the overall odour risk, it is necessary to deal with this issue in a dynamic manner. It is however difficult, expensive and not of particularly great value to try to quantify a wide range of these compounds.

The source term for odour is inherently time dependent. Odour enters the ventilated airspace from manure pit, and a substantial fraction of it is adsorbed to the existing aerosol to yield a size distribution of the dust-borne odour. Removal of dust-borne odour takes place by ventilation and by deposition (including turbulent diffusive deposition and gravitational sedimentation) onto walls and other surfaces. This is a competition between these factors that keep dust-borne odour airborne and those that remove dust-borne odour, and the relative effectiveness of the competing terms is functions of particle size and residence time. The model must keep track of this competition in each size range and update the dust-borne odour size distribution at each time step.

---

<sup>\*</sup> Corresponding author. Fax: +886-2-2362-6433.

E-mail address: hml@watgis.ae.ntu.edu.tw (C.-M. Liao)

Phenomena such as turbulent coagulation, diffusiophoresis and thermophoresis can also influence the dust-borne odour concentration [1,2]. The contributions from these effects, however, can be estimated to be small and are neglected in this model.

Generally, turbulent coagulation becomes very important for particles larger than 10  $\mu\text{m}$  [3] and the majority of dust particles found in animal housing have diameter ranged between 0.5 and 5  $\mu\text{m}$  [4,5]. There is some evidence of particles larger than 10  $\mu\text{m}$  found in swine nursery [6] but in a relative comparison with deposition and ventilation it reflects a insignificant contribution due to turbulent coagulation [1], and it is computationally expedient to neglect coagulation that leads to higher order contribution.

The concentration gradients are not expected to be large enough to make diffusiophoresis significant. The circulation of air in the model is considered as an isothermal condition, temperature gradients thus will not be established in the ventilation flow field and therefore that thermophoresis is not likely to be present. Additionally, there could be hygroscopic growth in the high humidity environment of the animal housing. Hygroscopic growth, however, is so rapid [3] that can be considered as a transient that occurs before odour adsorbs to the existing aerosol.

In this paper, the dynamic model is developed by using well-defined physical models for the underlying physical phenomena. Adsorption of the odour to the existing aerosol is relatively well understood and modeled using the formulas derived by Liao and Singh [7]. An adsorption rate concept thus could be refined from an adsorption model based on the homogeneous surface diffusion theory. Deposition is more complex. Even though diffusiophoresis and thermophoresis can be neglected, Brownian and turbulent diffusion, sedimentation and laminar as well as convective flow exist to varying degrees and lead to particle deposition onto walls and other surfaces.

Depending on the flow regime, different models have been proposed for particle deposition in a ventilated airspace. The turbulent flow scheme appears to be best applicable to a ventilated airspace in which turbulent flow is a typical feature of the airflow. A mathematical model derived by Crump and Seinfeld [8] for the rate of aerosol deposition on the walls of a turbulent mixing enclosure of arbitrary shape under the assumption of homogeneous turbulence near the walls was therefore adopted in the present work.

The goal of this work is to develop a conceptual framework for theoretical analysis to assess the relative importance of the variables that influence dynamic behavior of odour, airborne dust and dust-borne odour distributions and thus to extrapolate from limited experimental data to a range of possible distribution conditions. The input parameters to the model were varied to correspond to these factors and the model was applied to evaluate the range of possible conditions. A sensitivity analysis for evaluating the important parameters such as ventilation rate, airborne dust size and ambient aerosol profile in the ventilated airspace is also presented.

## 2. Model development

### 2.1. Dynamic equations

A ventilated airspace where the system boundary is taken as the walls, floor and ceiling of the enclosure is shown in Fig. 1. Fig. 1 illustrates the schematic diagram of the transport mechanisms and the components of the airborne dust-phase, gas-phase and adsorbed-phase. The dust generated from the floor and the odour emitted from the manure pit into the ventilated airspace are assumed to be instantaneously dispersed uniformly throughout the enclosure.

Before deriving the system dynamic equations to describe the concentration changes of airborne dust, odour and dust-borne odour over time within a ventilated airspace, the following

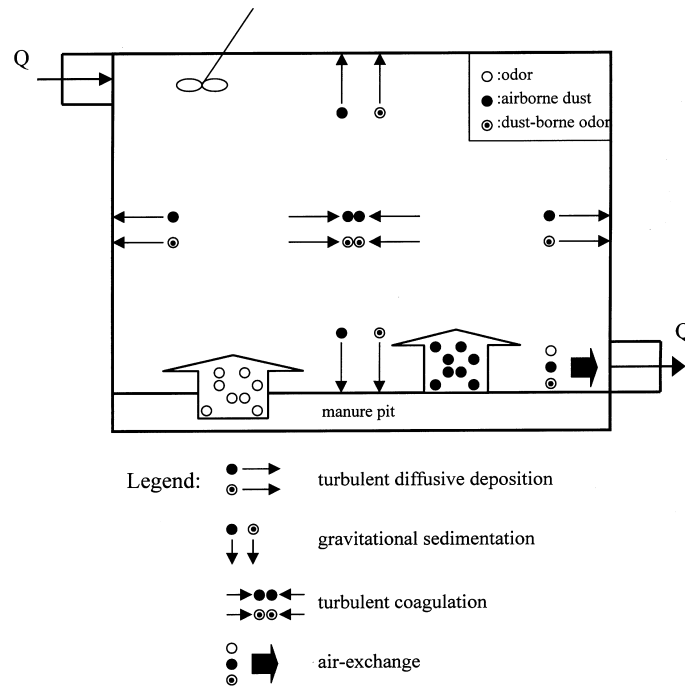


Fig. 1. Schematic diagram of the components of airborne dust, odour and dust-borne odour and their transport mechanisms in a ventilated airspace.

assumptions are made: (1) the ventilation airflow system is assumed to be a complete mixing system, (2) all odour ingredients are treated as one gas (i.e., bulk odour concentration), (3) a dust particle is treated as an aerodynamic equivalent sphere and is electrically neutral, (4) no gas-to-particle conversion occurs within the system, (5) mass transfer resistance from bulk odour to outer surface of dust particles and turbulent coagulation of dust- and adsorbed-phase are negligible, (6) bulk odour concentration is in equilibrium with the adsorbed phase concentration at the surface, and (7) odour is assumed to be adsorbed on the outer surface first, then enter the dust particle through surface diffusion, and eventually occupy adsorption sites in the inner surface.

From a micro-mixing point of view, the population-balance model is the basic model for a system describing the time- and size-dependent change in properties among airborne dust, odour and dust-borne odour undergoing adsorption between odour and airborne dust, turbulent diffusive deposition, gravitational sedimentation and ventilation airflow.

Gain and loss rates of the interaction among ambient aerosol, odour and dust-borne odour in a ventilated airspace based on the population-balance model is listed in Table 1. Mathematically, Table 1 can be written by the following dynamic equations in varying with particle size range  $k$  and time  $t$ ,

$$\frac{C_0(t)}{dt} = V^{-1}S(t) - \left( \lambda_v + \sum_{k=1}^{N-1} \lambda_a(k) \right) C_0(t), \quad (1)$$

$$\frac{C(k,t)}{dt} = \lambda_a(k)C_0(t) - (\lambda_v + \lambda_d(k))C(k,t), \quad k = 1, 2, \dots, N - 1, \quad (2)$$

Table 1

The gain and loss rates for the rate of change for odour, dust-borne odour and airborne dust in a ventilated airspace

Rate of change	Gain rate	Loss rate
Odour concentration at time $t$	Odour source strength emitted from manure pit	1. Air exchange rate 2. Adsorption rate of odour to aerosol surface for all size ranges
Dust-borne odour with size range $k$ and at time $t$	Adsorption rate of odour to aerosol surface	1. Air exchange rate 2. Deposition rate of turbulent diffusive deposition and gravitational settling at size range $k$
Airborne dust concentration with size range $k$ and at time $t$	Dust source strength generated from floor due to air exchange rate	1. Deposition rate of turbulent diffusive deposition and gravitational settling at size range $k$ 2. Air exchange rate 3. Loss rate of aerosol being transformed to dust-borne odour

$$\frac{dn(k, t)}{dt} = -\lambda_d(k)n(k, t) + \lambda_v(n_s(k, t) - n(k, t)) - \gamma C(k, t), \quad k = 1, 2, \dots, N-1, \quad (3)$$

where  $C_0(t)$  is the time-dependent odour concentration ( $\text{kg m}^{-3}$ );  $S(t)$  the odour source strength ( $\text{g s}^{-1}$ );  $V$  the air volume ( $\text{m}^3$ );  $\lambda_v$  the air exchange rate ( $\text{s}^{-1}$ ) in which  $\lambda_v = Q/V$ ,  $Q$  the ventilation rate ( $\text{m}^3 \text{s}^{-1}$ );  $C(k, t)$  the time-dependent dust-borne odour concentration in the  $k$ th size range ( $\text{kg m}^{-3}$ );  $\lambda_a(k)$  the rate of adsorption of odour to aerosol surface in the  $k$ th size range ( $\text{s}^{-1}$ );  $\lambda_d(k)$  the deposition rate of dust-borne odour or aerosol due to turbulent diffusive and gravitational sedimentation in the  $k$ th size range ( $\text{s}^{-1}$ );  $n(k, t)$  the time-dependent aerosol concentration in the  $k$ th size range ( $\text{kg m}^{-3}$ );  $n_s(k, t)$  the source concentration of dust in the  $k$ th size range ( $\text{kg m}^{-3}$ );  $\gamma$  the loss rate of aerosol being transformed to dust-borne odour ( $\text{s}^{-1}$ );  $k$  the size range number; and  $N$  is assigned to be the end point number for a  $k$ th size range,  $d_k$  and  $d_{k+1}$ .

In the present analysis, the particle is divided by geometrically equal size bin in the size range of interest. The dust-borne odour or aerosol concentration is assumed to be a constant diameter within a bin. The end points,  $d_k$  and  $d_{k+1}$ , of the  $k$ th size bin are considered to be equal to the logarithmic mean of the end points of the bin as,

$$\ln d_k = \ln d_{\min} + \frac{(\ln d_{\max} - \ln d_{\min})(k-1)}{N-1}, \quad k = 1, 2, \dots, N, \quad (4)$$

where particles smaller than  $d_{\min}$  are considered to be the finest, and  $d_{\max}$  is the largest particle size of interest.

## 2.2. Odour source strength

The scenario of the stored manure pit can be described as follows: (1) the contaminated source is uniformly distributed in a thickness  $W$  of the contaminated layer, (2) odour in the contamination zone diffuses up through a clean layer of thickness  $L$  of manure slurry, (3) the chemicals move in one dimension through the pig slurry in accordance with the principle of mass balance, and (4) pig slurry is assumed to be isotropic and homogeneous.

The volatilization odour flux from stored manure pit of chemical located initially between  $L$  and  $L+W$  can then be described by the following equation [9],

$$J_s(t) = C_s e^{-\mu t} \left( \frac{D_E}{\pi t} \right)^{1/2} \left[ \exp\left( \frac{-L^2}{4D_E t} \right) - \exp\left( \frac{-(L+W)^2}{4D_E t} \right) \right], \quad t > 0, \quad (5)$$

where  $J_s(t)$  is the time-dependent odour flux from manure pit ( $\text{g m}^{-2} \text{s}^{-1}$ ),  $C_s$  the initial odour concentration in slurry column ( $\text{g m}^{-3}$ ),  $\mu$  the first-order degradation rate constant of chemical ( $\text{d}^{-1}$ ),  $L$  the clean layer thickness of slurry (m),  $W$  the contaminated layer thickness of slurry (m) and  $D_E$  is the effective diffusion coefficient of odour in the slurry ( $\text{m}^2 \text{s}^{-1}$ ).

The time-dependent odour source strength therefore have the following form as,

$$S(t) = J_s(t)A, \quad (6)$$

where  $A$  is the manure pit area ( $\text{m}^2$ ).

Eq. (5) has been used to evaluate indoor inhalation exposure dynamics of odour causing volatile organic compounds volatilization from stored pig slurry [10]. The key parameter in Eq. (5) is the effective diffusion coefficient. According to the model developed by Jury et al. [9], the effective diffusion coefficient defines the rate of mass transfer between the liquid and gas phases. Thus  $D_E$  depends on the combined mass transfer through liquid and gas boundary layers.

### 2.3. Adsorption rate

In a paper addressing the adsorption of odour to the surface of existing airborne dust in swine housing based on age and size distributions of dust particle [7], a homogeneous surface diffusion theory is used to evaluate the dust-borne odour dynamics in a ventilated enclosure. Based on the formulas derived by Liao and Singh (referred to as L–S model) [7], the concept of adsorption coefficient which has a unit as airflow rate in  $\text{m}^3 \text{s}^{-1}$  can be obtained. The L–S model, however, must be applied with caution because they were based only on a theoretical analysis but little empirical justification.

When applying an overall steady-state mass balance equation on the bulk odour and adsorbed dust-borne odour phases yields the following equation [7]:

$$\beta(d_p)C_{0,e} = w_e \eta[\Phi(d_p)]q, \quad (7)$$

where  $\beta(d_p)$  is the adsorption coefficient of odour to the surface of an airborne dust with diameter  $d_p$  ( $\text{m}^3 \text{s}^{-1}$ ),  $C_{0,e}$  the steady-state odour concentration ( $\text{kg m}^{-3}$ ),  $w_e$  the amount adsorbed in equilibrium with bulk odour concentration ( $\text{kg kg}^{-1}$ ),  $q$  the airborne dust exchange rate ( $\text{kg s}^{-1}$ ) and  $\eta[\Phi(d_p)]$  is the size-dependent effectiveness factor (dimensionless) in which  $\Phi(d_p)$  is a size-dependent diffusion length modulus (dimensionless), and could be expressed respectively as [7],

$$\eta[\Phi(d_p)] = \frac{3}{\Phi^2(d_p)} (\Phi(d_p) \coth(\Phi(d_p)) - 1), \quad (8)$$

$$\Phi(d_p) = \frac{d_p}{\sqrt{D_s \bar{\tau}}}, \quad (9)$$

where  $D_s$  is the surface effective diffusivity of odour in the air ( $\text{m}^2 \text{s}^{-1}$ ),  $\sqrt{D_s \bar{\tau}}$  can be seen as a diffusion length of odour (cm) and  $\bar{\tau}$  is the mean residence time of ventilation air ( $\bar{\tau} = V/Q$ ) (h).

If the adsorption reaction of the equilibrium odour concentration at the outer surface of a dust particle is described by means of a Freundlich isotherm, the final expression of the adsorption coefficient  $\beta(d_p)$  could be obtained from Eq. (7) as,

$$\begin{aligned}\beta(d_p) &= \frac{w_e \eta [\Phi(d_p)] q}{C_{0,e}} = \frac{K C_{0,e}^m \eta [\Phi(d_p)] q}{C_{0,e}} \\ &= K C_{0,e}^{m-1} \left( \frac{3}{\Phi^2(d_p)} (\Phi(d_p) \coth(\Phi(d_p)) - 1) \right) Q \rho_p,\end{aligned}\quad (10)$$

where  $\rho_p$  is the density of dust particle ( $\text{kg m}^{-3}$ ), and  $K$  ( $(\text{m}^3 \text{kg}^{-1})^m$ ) as well as  $m$  ( $m > 0$ ) are constants of the Freundlich isotherm and could be determined empirically from independent equilibrium experiments.

Airborne dust particles in animal housing are usually not homogeneous in size [1,2]. Sieve analysis is often performed to determine a particle size distribution in terms of various size fractions [4]. The rate of adsorption of odour to an airborne dust surface,  $\lambda_a(k)$  ( $\text{s}^{-1}$ ) therefore could be expressed as

$$\lambda_a(k) = Z \int_{d_k}^{d_{k+1}} \beta(d_p) f(d_p) d(d_p), \quad (11)$$

where  $f(d_p)$  is the airborne dust size distribution function and  $Z$  is the total airborne dust concentration ( $\text{particles cm}^{-3}$ ). The total adsorption rate is obtained by summing the contribution from all the size bins.

The lognormal distribution is the most common used distribution for characterizing aerosol particle size [3,6]. The mathematical form of a particle size distribution thus can be obtained using a lognormal distribution model [6],

$$f(d_p) d(d_p) = \frac{1}{\sqrt{2\pi} \ln \sigma_g} \exp\left(-\frac{(\ln d_p - \ln d_g)^2}{2(\ln \sigma_g)^2}\right) d(\ln d_p) \quad (12)$$

with a geometric mean diameter  $d_g$  and a geometric standard deviation  $\sigma_g$ . These parameters are varied to correspond to the typical aerosol profiles found in the animal housing. Experimentally measured particle size distributions could also be used as input for the computation of the adsorption rate.

#### 2.4. Deposition rate

A well-established general model for the rate of aerosol deposition due to turbulent diffusion, Brownian diffusion and gravitational sedimentation in a turbulently mixed, enclosed enclosure of arbitrary shape is derived by Crump and Seinfeld [8], and is referred to as the C–S model.

Application of the C–S model to a rectangular enclosure yields expression for the deposition rate,  $\lambda_d(d_p)$ , of a particle of diameter,  $d_p$ ,

$$\begin{aligned}\lambda_d(d_p) &= \frac{1}{lwh} \left\{ (2wh + 2hl) \left[ \left( \sin \frac{\pi}{n} \right) \left( k_e D(d_p)^{n-1} \right)^{1/n} \right] \right. \\ &\quad \left. + wlv_s(d_p) \coth \left( \frac{\pi v_s(d_p)}{2(n \sin \frac{\pi}{n}) \left( k_e D(d_p)^{n-1} \right)^{1/n}} \right) \right\},\end{aligned}\quad (13)$$

where  $D(d_p)$  and  $v_s(d_p)$  are the Brownian diffusion coefficient ( $\text{m}^2 \text{s}^{-1}$ ) and the settling velocity ( $\text{m s}^{-1}$ ) of a particle of diameter  $d_p$ , respectively;  $n$  and  $k_e$  are used to calculate the eddy diffusion

coefficient; and  $l$ ,  $w$ , as well as  $h$  are the length, width and height of the enclosure. The deposition rate is assumed to be species independent.

The Brownian diffusion coefficient of a particle of diameter,  $d_p$ , is

$$D(d_p) = \frac{k_B T C_{\text{slip}}}{3\pi\eta_a d_p}, \quad (14)$$

where  $k_B$  is the Boltzmann constant ( $1.380 \times 10^{-16}$  erg  $\text{K}^{-1}$ ),  $T$  the ambient absolute temperature (K),  $\eta_a$  the dynamic viscosity of air (p) and  $C_{\text{slip}}$  is the slip correlation factor (dimensionless) [11],

$$C_{\text{slip}} = \left\{ 1 + \frac{\lambda}{d_p} \left[ 2.541 + 0.8 \exp\left(-0.55 \frac{d_p}{\lambda}\right) \right] \right\}, \quad (15)$$

where  $\lambda$  is the mean free path of air (cm).

The settling velocity of a particle of diameter,  $d_p$ , is

$$v_s(d_p) = \frac{\rho_p g d_p^2}{18\eta_a} C_{\text{slip}} \left( 1 - \frac{\rho_a}{\rho_p} \right), \quad (16)$$

where  $\rho_a$  is the density of the air ( $\text{g cm}^{-3}$ ),  $\rho_p$  the particle density ( $\text{g cm}^{-3}$ ) and  $g$  is the gravitational acceleration constant ( $\text{m s}^{-2}$ ). The deposition rate for the  $k$ th size bin is obtained by integrating Eq. (13) over the whole bin,

$$\lambda_d(k) = \frac{1}{d_{k+1} - d_k} \int_{d_k}^{d_{k+1}} \lambda_d(d_p) d(d_p). \quad (17)$$

The C–S model was developed for reactor vessels where turbulence is produced by stirring. The turbulence parameter ( $k_e$ ) was estimated by assuming complete turbulent dissipation of the input energy. In the case of ventilation-induced turbulence, however, it is difficult to estimate  $k_e$ . In the present analysis, the estimates of  $k_e$  used were obtained from the work by Nazaroff and coworkers [12,13] in that the range of variations of  $k_e$  in indoor air was based on airflow velocity scheme in the room. The analysis was also applied to a chamber where mixing fans are present and a semi-empirical expression derived for  $k_e$  based on a fan specification [14].

### 3. Numerical simulation

#### 3.1. Input parameters

A typical pig unit measuring  $6 \times 2.5 \times 2.4 \text{ m}^3$  with a totally slatted floor is chosen for illustrative purpose of modeling. This unit has one negative pressure ventilation system of one high endwall exhaust fans with a continuous slot inlet. The body weight of each growing pig was estimated to be 70 kg.

The system of Eqs. (1)–(3) is a linear, first-order system of coupled differential equations. Integration over time is straightforward in principle but is complicated by the existence of a large number of widely differing time scales. The numerical integration scheme used to solve the system dynamic Eqs. (1)–(3) is a subroutine DIVPRK [15] based on the Runge–Kutta–Verner 5th-order and 6th-order method and done in double precision with FORTRAN 77. The algorithm is stable provided the error and the convergence criterion are carefully monitored.

The parameters used in the model simulation are listed in Table 2. Table 2 shows the ambient temperature is held fixed at  $25^\circ\text{C}$ . Calculations using the model developed for this work indicate

Table 2  
Input parameters for the model simulation

Parameter	Description	Representation values
<i>Odour source strength<sup>a</sup></i>		
$D_E$	Effective diffusion coeff. of odour	$2.25 \times 10^{-9} \text{ m}^2 \text{ s}^{-1}$
$L, W$	Clean and contaminated layers thickness	$L = 1 \text{ cm}, W = 10 \text{ cm}$
$A$	Manure pit area	$6 \times 3.5 \text{ m}^2$
$\mu$	1st order degradation rate	$3.15 \times 10^{-2} \text{ d}^{-1}$
$C_s$	Initial odour concen. in slurry	$5 \text{ mg l}^{-3}$
<i>Adsorption rate</i>		
$D_s$	Surface effective diffusivity of odour in air	$1.27 \times 10^{-8} \text{ m}^2 \text{ s}^{-1\text{b}}$
$K, m$	Parameters of Freundlich isotherm	$K = 0.2, m = 1$
$V = lwh$	Enclosure dimension	$l = 6 \text{ m}, w = 2.5 \text{ m}, h = 2.4 \text{ m}$
<i>Deposition rate</i>		
$n$	Exponent constant	$2^c$
$k_e$	Turbulent intensity parameter	$0.1 \text{ s}^{-1\text{c}}$
$\eta_a$	Dynamic viscosity of air	$1.8 \times 10^{-3} \text{ P}^d$
$\rho_a$	Density of air	$1.2 \times 10^{-3} \text{ g cm}^{-3\text{d}}$
$K_B$	Boltzmann's constant	$1.38 \times 10^{-16} \text{ erg K}^{-1\text{d}}$
$T$	Ambient temperature	$25^\circ\text{C}$
$\lambda$	Mean free path of air	$0.66 \times 10^{-5} \text{ cm}^d$
$\rho_p$	Particle density	$1.0 \text{ g cm}^{-3}$

<sup>a</sup> Adapted from Liao et al. [10].

<sup>b</sup> Adapted from Liao and Singh [7].

<sup>c</sup> Adapted from Nazaroff et al. [13].

<sup>d</sup> Adapted from Hinds [3].

that, ignoring thermophoretic forces, a change in temperature from 10°C to 35°C has an negligible effect on the adsorption and deposition rates. Due to the goal of this work, to examine the dynamic behavior of the dust-borne concentration, the initial conditions for the gas-, adsorbed- and particle-phase concentrations for all the simulations were assumed to be zero.

Two different size ranges were considered accounting for a sampling of airborne dust produced by particle sources found in animal housing: a 0.5–5  $\mu\text{m}$  and a 0.52–21.3  $\mu\text{m}$  as measured in a swine growing house [4] and a swine nursery [6], respectively.

In order to find an equivalent geometrical standard deviation (gsd) representing the swine dust particle size distribution with a known geometrical mean diameter (gmd) of 2  $\mu\text{m}$  based on the measurements by Gao and Feddes [4], a lognormal distribution model shown in Eq. (9) was used to find an equivalent size distribution by try and error to match an experimental measurement. The result is shown in Fig. 2A and the equivalent gsd is 1.65.

Maghirang et al. [6] showed that the lognormal distribution can be used to fit the daily particle size distribution in a mechanically ventilated swine nursery during warm weather conditions and a gsd of 3 was found (Fig. 2B). A gmd in the lognormal size distribution however needs to be determined. A calculation based on the particle data adopted from Maghirang et al. [6] yields an equivalent 8  $\mu\text{m}$  gmd. The size-dependent dust source concentrations on the floor shown in Table 3 were calculated based on a dust size distribution illustrated in Fig. 2.

Table 3 summarizes the operating parameters used in the model simulations. The ambient aerosol profile, however, was assumed to be time-independent during each individual simulation.

The Freundlich isotherm is widely used to describe sorption equilibrium in environmental systems with heterogeneous surfaces. Although, in this paper airborne dust is superficially assumed as homogeneous materials, significant heterogeneity likely exists. Additionally, over time, airborne dust surface slowly reacted by means of physicochemical or biological manners, which



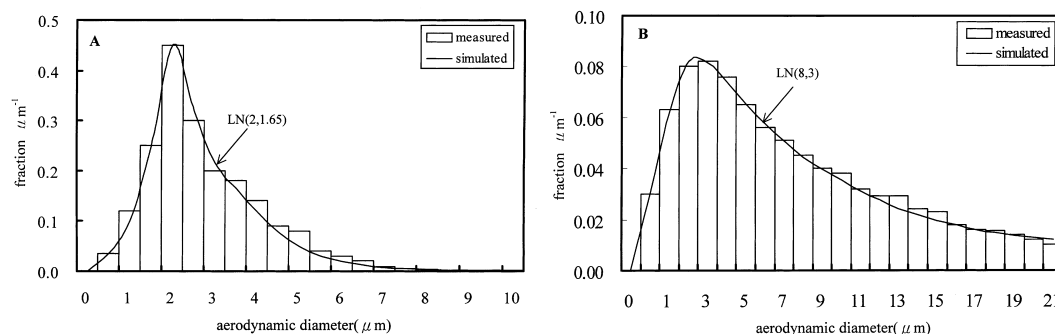


Fig. 2. Measured and simulated particle size distributions for: (A) a swine growing house with 2  $\mu\text{m}$  gsd, 1.65 gmd and 3 gmd (B) a swine nursery with 8  $\mu\text{m}$  gsd, 3 gmd.

Table 3  
Operating parameters used in the model simulation

Ventilation rate ( $\text{m}^3 \text{h}^{-1}$ )					
280					
845					
1440					
gmd ( $\mu\text{m}$ )	gsd	Z (particle $\text{cm}^{-3}$ )			
Aerosol profile					
2 <sup>a</sup>	1.65 <sup>b</sup>	1000 <sup>c</sup>			
8 <sup>b</sup>	3 <sup>d</sup>	5000 <sup>c</sup>			
	Bin number				
	1	2	3	4	5
Dust source concentration in each bin (particle $\text{cm}^{-3}$ )					
gmd = 2 $\mu\text{m}$	120 (0.95) <sup>e</sup>	450 (1.85)	200 (2.75)	150 (3.65)	80 (4.55)
gmd = 8 $\mu\text{m}$	600 (2.55)	2250 (6.65)	1000 (10.75)	750 (14.85)	400 (18.95)

<sup>a</sup> Adapted from Gao and Feddes [4].

<sup>b</sup> Calculated from Eq. (9).

<sup>c</sup> Estimated values based on Fig. 2.

<sup>d</sup> Adapted from Maghirang et al. [6].

<sup>e</sup> Numbers in parentheses are average particle diameter in micrometer of each size bin.

may further contributed to surface heterogeneity. Often one finds  $0 < m \leq 1$  for Freundlich exponents in Eq. (10). An  $m = 1$  (i.e., a linear isotherm) is used in present analysis to simplify the model simulation for expedient computation. Van Loy et al. [16] however have shown that the linear model correctly captures the dynamics of volatile compounds sorption on indoor materials.

### 3.2. General results

Fig. 3 shows a simulation result of the typical time evolution of concentration profiles for odour (Fig. 3A), airborne dust (Fig. 3B) and dust-borne odour for swine dust with gmd 2  $\mu\text{m}$ , gsd 1.65, 1000 particle  $\text{cm}^{-3}$ , and ventilation rate is 845  $\text{m}^3 \text{h}^{-1}$ . The contribution to the concentration profiles from each size bin is also shown.

Fig. 3B indicates that the dust-borne odour in bins 2 and 3 the effects of adsorption is greater than that of deposition due to smaller particles, while there is a balancing competition between deposition and adsorption in bins 1 and 4. For the larger particles in bin 5 deposition always takes control. Fig. 3C shows that there exists competition between deposition and adsorption in bins 3

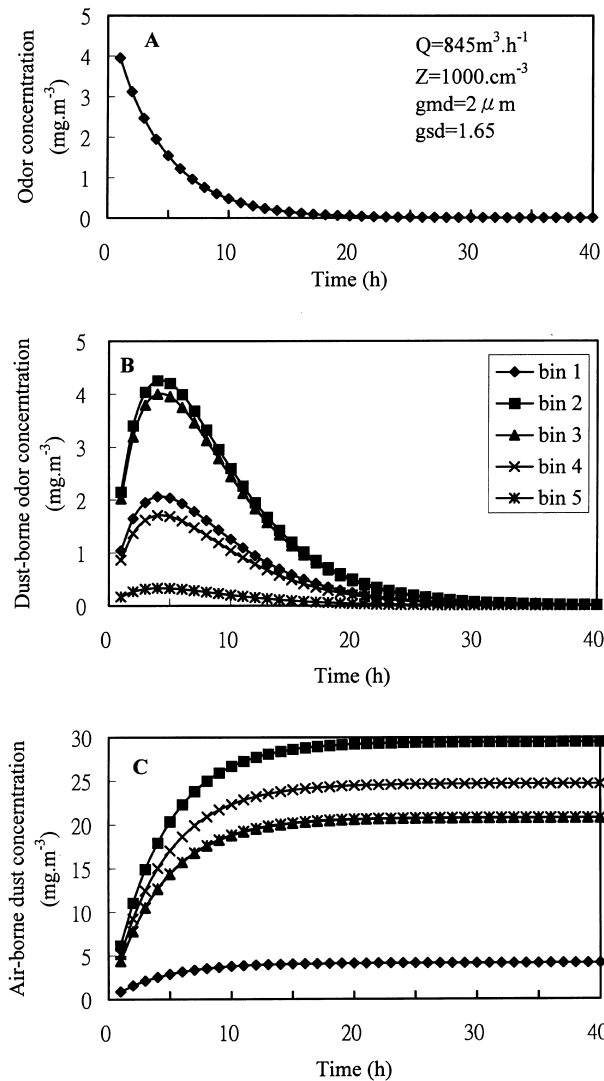


Fig. 3. Simulation result for a typical time evolution of concentration profiles of odour, dust-borne odour and airborne dust with  $2\ \mu\text{m}$  gsd,  $1.65\ \text{gmd}$ ,  $1000\ \text{particles cm}^{-3}$  and ventilation rate is  $845\ \text{m}^3\ \text{h}^{-1}$ .

and 4. The deposition effect in airborne dust is a loss rate as a result of aerosol being transformed to a dust-borne odour.

Table 4 gives the simulation results of adsorption and deposition rates for two different aerosol profiles under a ventilation rate of  $845\ \text{m}^3\ \text{h}^{-1}$ . Table 4 indicates that the orders of magnitude of adsorption and deposition rates for  $\text{gmd}$  of 2 and  $8\ \mu\text{m}$  aerosol are  $10^{-2}$  and  $10^{-3}\ \text{h}^{-1}$  respectively. This effect is shown in the Eq. (10) in which  $\beta(d_p)$  and  $d_p^{-1}$  is directly proportional. The average orders of magnitude of deposition rates for 2 and  $8\ \mu\text{m}$   $\text{gmd}$  aerosol are  $10^{-3}$  and  $10^{-2}\ \text{h}^{-1}$ , respectively.

### 3.3. Effect of ventilation rate

Fig. 4 shows a simulation where the ventilation rate was varied from  $280$  to  $1440\ \text{m}^3\ \text{h}^{-1}$  for a  $2\ \mu\text{m}$   $\text{gmd}$  aerosol and the particle concentration is  $1000\ \text{cm}^{-3}$ . As expected the peak dust-borne

Table 4

Simulation results of adsorption and deposition rates for two different aerosol profiles ( $Q = 845 \text{ m}^3 \text{ h}^{-1}$  and  $Z = 1000 \text{ cm}^{-3}$ )

	Bin number ( $k$ )	Adsorption rate ( $\lambda_a(k)$ , $\text{h}^{-1}$ )	Deposition rate ( $\lambda_d(k)$ , $\text{h}^{-1}$ )	$\lambda_a(k)/\lambda_d(k)$
gmd = 2 $\mu\text{m}$ , gsd = 1.65	1	$2.63 \times 10^{-2}$	$5.35 \times 10^{-4}$	49.16
	2	$5.44 \times 10^{-2}$	$5.49 \times 10^{-4}$	99.09
	3	$5.12 \times 10^{-2}$	$1.22 \times 10^{-3}$	41.97
	4	$2.18 \times 10^{-2}$	$5.92 \times 10^{-3}$	3.68
	5	$4.21 \times 10^{-3}$	$3.59 \times 10^{-2}$	$1.20 \times 10^{-1}$
gmd = 8 $\mu\text{m}$ , gsd = 3	1	$1.86 \times 10^{-2}$	$5.26 \times 10^{-4}$	35.31
	2	$1.47 \times 10^{-2}$	$1.40 \times 10^{-3}$	10.52
	3	$7.47 \times 10^{-3}$	$2.16 \times 10^{-2}$	$3.46 \times 10^{-1}$
	4	$2.42 \times 10^{-3}$	$4.25 \times 10^{-1}$	$5.70 \times 10^{-3}$
	5	$5.02 \times 10^{-4}$	5.19	$1.00 \times 10^{-4}$

odour concentration is smaller at higher ventilation rates. Additionally, the peak occurs earlier as the ventilation increases.

This pattern was also seen in the odour and airborne dust concentration profiles in that the equilibrium occurs earlier as the ventilation increases. As the ventilation rate increases, the time to reach the maximum concentration decreases, and the maximum concentration decreases. Therefore, increased ventilation rate not only lowers maximum dust-borne odour concentration but it also causes the maximum concentration to be reached in a shorter time.

Results obtained thus suggest that the role of ventilation as an effective removal technique is of fundamental and practical significance.

### 3.4. Effect of aerosol profile

Fig. 5 shows simulations performed for two different aerosol profiles and a ventilation rate of  $845 \text{ m}^3 \text{ h}^{-1}$ . Fig. 5 indicates the smaller particle diameter leads to greater adsorption, which keeps the dust-borne odour airborne. The larger particles are more effectively removed by deposition. Therefore, changes in particle size to a larger size could lower maximum dust-borne odour concentrations. The reducing of dust-borne odour concentration of each size bin in Fig. 5 is followed by a decreasing order of magnitudes of adsorption rates shown in Table 4.

The effects of particle concentration are also presented. Fig. 5A and B give simulations for a 2  $\mu\text{m}$  gmd and 1.65 gsd aerosol profile at particle concentration of 1000 and 5000  $\text{cm}^{-3}$  respectively, while the performance for a 8  $\mu\text{m}$  gmd and 3 gsd aerosol at 5000 and 1000  $\text{cm}^{-3}$  is illustrated in Fig. 5C and D. Fig. 5 show that the more larger amount of particle concentration also leads to greater adsorption and keeps the dust-borne odour airborne. A comparisons between Fig. 5A and B as well as between Fig. 5C and D, it is found that, to a very good level of approximation, the dust-borne odour concentrations varies directly proportional as the particle concentration. This is to be expected since the adsorption rate is directly proportional to the particle concentration (Eq. (11)).

The most important implication of the changes in particle size will have two effects. First, the changes in the sizes will affect the deposition of the particles onto the enclosure surface and thus affect the amount of dust-borne odour products available for inhalation. Second, the changes in size will alter where the particles deposit within the respiratory tract. Additionally, if the number of particles is relatively small, adsorption is low and the dominant contribution to the exposure dose for workers and animals is from the fine dust.

The consideration of size distribution is important to the study in exposure dose assessment due to its sensitivity on the size of the inhaled particle carrying odour. It is worth to note that the

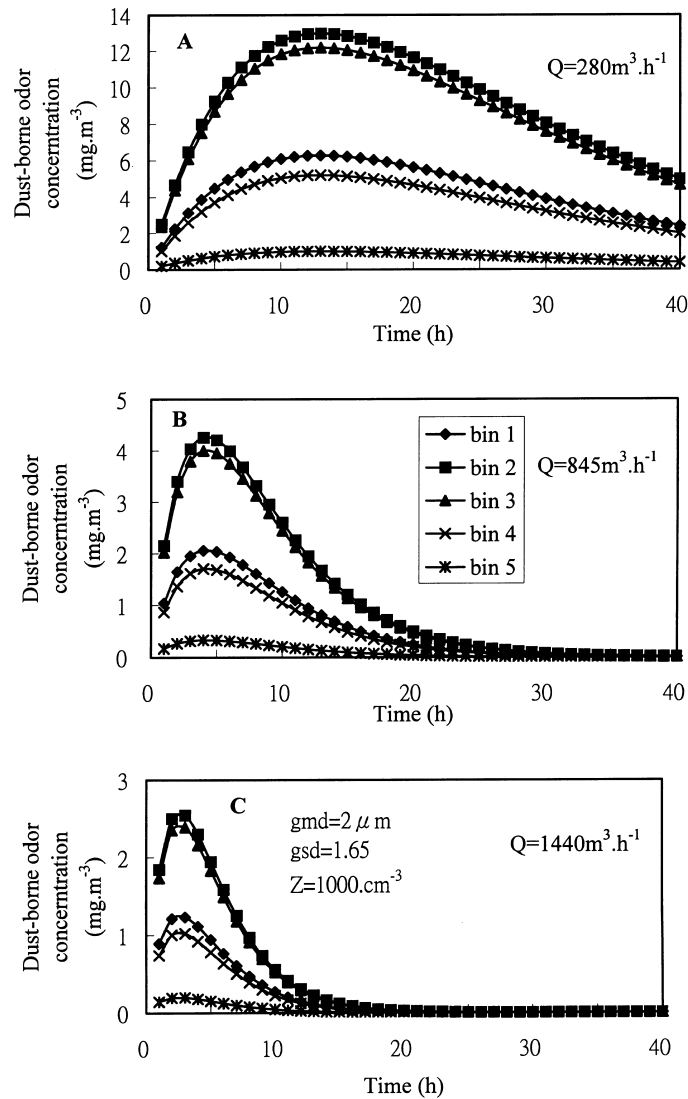


Fig. 4. Simulation result where ventilation rate was varied from 280 to 1440  $\text{m}^3 \text{ h}^{-1}$  for a  $2 \mu\text{m}$  gsd with 1.65 gmd aerosol and particle concentration is 1000 particles  $\text{cm}^{-3}$ .

ambient aerosol may undergo some hygroscopic growth in the high humidity environment in animal housing, e.g., in a misting system. If the aerosol particle can grow to a large size, then this increase will result in a large adsorption rate of dust-borne odour. Also if the aerosol can grow in the high humidity achieved during misting, then it can grow in the respiratory tract. Therefore, when the dust-borne odour enters the lung is reduced, the amount of possible growth depends on how close the relative humidity in animal housing is to 100% and further alters the deposition patterns within the lung.

### 3.5. Effect of enclosure dimensions

Simulations were also performed for the three different size enclosures measured in surface to volume ratio of 0.5, 1 and 2. It was found that the changes in dust-borne odour concentration due to the changes in surface to volume ratio varied insignificantly.

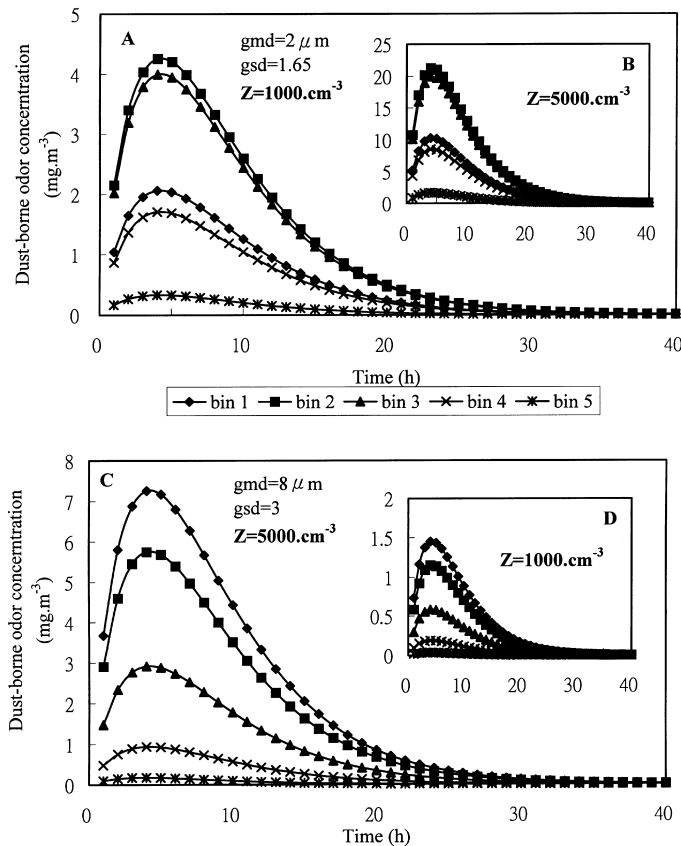


Fig. 5. Simulation performances for two different aerosol profiles: (A)  $gmd = 2$ ,  $gsd = 1.65$ ,  $Z = 1000 \text{ cm}^{-3}$ , (B)  $gmd = 2 \mu\text{m}$ ,  $gsd = 1.65$ ,  $Z = 5000 \text{ cm}^{-3}$ , (C)  $gmd = 8 \mu\text{m}$ ,  $gsd = 3$ ,  $Z = 5000 \text{ cm}^{-3}$  and (D)  $gmd = 8 \mu\text{m}$ ,  $gsd = 3$ ,  $Z = 1000 \text{ cm}^{-3}$ .

From a theoretical point of view, as the enclosure volume decreases, its surface to volume ratio increases, and this leads to a higher rate of deposition of particles. There is an additional factor that the dust-borne odour concentration varies inversely as the volume of the enclosure. The consequent values however are small for the expected variation in enclosure volume. For reasons of no variations in output figures, those simulations are not presented here.

#### 4. Conclusions

Although, the modeling study has to use the experimental work to verify its feasibility, it has not been possible to make a direct comparison with an experiment since dynamic measurements are not available for the size distribution of the dust-borne odour concentrations. The model therefore provides a theoretical framework to extrapolate beyond the immediate experimental results.

A series of sensitivity analysis were made to illustrate the effects of the aerosol profile, enclosure dimension, and ventilation rate on dust-borne odour concentration and to demonstrate the usefulness of the model for evaluating the performance of a ventilation system for animal housing. Increased ventilation rate and a reduction of total airborne dust concentration are both found to be highly effective in dust-borne odour concentration reduction. The smaller particle diameter keeps the dust-borne odour airborne, while the larger particles are more effectively

removed by deposition, and hence, an increase of the size of airborne dust can reduce the dust-borne odour concentration.

Results obtained indicate that the particle size distribution of dust-borne odour in a ventilated airspace is maintained in a relatively steady-state condition by turbulent diffusive deposition and gravitational sedimentation at deposition rates of  $10^{-3}$  and  $10^{-2}$   $\text{h}^{-1}$  order, while by adsorption of odour to airborne dust surface at deposition rates of  $10^{-2}$  and  $10^{-3}$   $\text{h}^{-1}$  order, respectively for 2 and 8  $\mu\text{m}$  gmd aerosol.

Although particles smaller than 1–2  $\mu\text{m}$  made up less than 30–40% of the total particle concentration in swine housing, they contributed significantly to the available adsorption surface area. Because particles of this size are expected to keep the dust-borne odour airborne and be transported with the airflow, they may be important to the fate of both organic- and bio-aerosol.

This analysis capability has crucial environmental implications. For instance, the dynamics approach presented in this study can be applied to more complex indoor air pollution systems such as the inhalation exposure from the radon in the water in homes, the health effects of ambient tobacco smoke and the health risk assessment of residential wood combustion.

### Acknowledgements

The authors wish to acknowledge the financial support of the National Science Council of Republic of China under Grant NSC 88-2621-B-002-005.

### References

- [1] C.M. Liao, J.J.R. Feddes, Modelling and analysis of airborne dust removal from a ventilated airspace, *Canadian Agric. Eng.* 33 (1991) 355–361.
- [2] C.M. Liao, J.J.R. Feddes, A lumped-parameter model for predicting airborne dust concentration in a ventilated airspace, *Trans. ASAE* 35 (1992) 1973–1978.
- [3] W.C. Hinds, *Aerosol Technology*, Wiley, New York, 1982.
- [4] W. Gao, J.J.R. Feddes, Using swine dust to verify a lumped-parameter model in a ventilated enclosure, *Canadian Agric. Eng.* 35 (1993) 67–73.
- [5] G.L. Van Wicklen, M.F. Yoder, Respirable aerosol concentrations in an enclosed swine nursery, *Trans. ASAE* 31 (1988) 1798–1803.
- [6] R.G. Maghirang, M.C. Puma, Y. Liu, P. Clark, Dust concentrations and particle size distribution in an enclosed swine nursery, *Trans. ASAE* 40 (1997) 749–754.
- [7] C.M. Liao, S. Singh, Modeling dust-borne dust dynamics in swine housing based on age and size distributions of airborne dust, *Appl. Math. Modelling* 22 (1998) 671–685.
- [8] J.G. Crump, J.H. Seinfeld, Turbulent deposition and gravitational sedimentation of an aerosol in a vessel of arbitrary shape, *J. Aerosol Sci.* 12 (1981) 405–415.
- [9] W.A. Jury, D. Russo, G. Streile, H.E. Abd, Evaluation of volatilization by organic chemicals residing below the soil surface, *Water Resour. Res.* 26 (1990) 13–20.
- [10] C.M. Liao, H.M. Liang, S. Singh, Exposure assessment model for odour causing VOCs volatilization from stored pig slurry, *J. Environ. Sci. Health B* 33 (1998) 457–486.
- [11] C.N. Davies, Deposition from moving aerosols, in: C.N. Davies (Ed.), *Aerosol Sciences*, Academic Press, New York, 1966, pp. 393–446.
- [12] W.W. Nazaroff, G.R. Cass, Mass-transport aspects of pollutant removal at indoor surfaces, *Environ. Int.* 15 (1989) 567–584.
- [13] W.W. Nazaroff, M.P. Ligocki, T. Ma, G.R. Cass, Particle deposition in museums: comparison of modeling and measurement results, *Aerosol Sci. Tech.* 13 (1990) 332–348.
- [14] K. Okuyama, Y. Kousaka, S. Yamamoto, T. Hosokawa, Particle loss of aerosols with particle diameters between 6 and 2000 nm in stirred tank, *J. Colloid Interface Sci.* 110 (1986) 214–223.

- [15] IMSL MATH/LIBRARY. FORTRAN Subroutine for Mathematical Applications, vol. 1, Visual Numerics, Houston, Texas, 1994.
- [16] M.D. Van Loy, V.C. Lee, L.A. Gundel, J.M. Daisey, R.G. Sextro, W.W. Nazaroff, Dynamic behavior of semivolatile organic compounds in indoor air 1. Nicotine in a stainless steel chamber, *Environ. Sci. Tech.* 31 (1997) 2554–2561.